Analysis of the Motion of a Ball in the Barrel of a Musket

Carl E. Mungan and John S. Denker

U.S. Naval Academy, Annapolis, MD

Abstract

The one-dimensional motion of a particle is analyzed when the force on it is inversely proportional to its displacement and directly proportional to the elapsed time. Such a force law describes a projectile in a musket barrel that is propelled by a hot ideal gas where either the number of moles or the temperature increases linearly with time due to the burning gunpowder. A particular solution to Newton's second law is found analytically for the case of zero initial position and velocity. For more general initial conditions, numerical integration is used to find the position of the particle as a function of time. A scaling argument shows that at long times, these numerical general solutions all converge to the analytic particular solution. Further analysis reveals how that convergence occurs: the general solutions slowly oscillate about the particular solution with a predictable period and amplitude. In addition to the dynamics, the energetics of the motion are analyzed.

Basic Dynamics of the Ball in a Musket

A LEAD BALL of mass m is tamped down the barrel of a musket of cross-sectional area A, so that it rests against a layer of black powder with initial position $x_0 = 0$ and velocity $\upsilon_0 = 0$, as sketched in Figure 1. Model the system by making three assumptions that simplify the analysis and bring out its essential features. First, suppose [1] the powder burns at a constant rate r, creating n moles of hot gas at temperature T as a function of time t, so that

$$n = rt\,. \tag{1}$$

Second, assume that the gas expands isothermally [2] as the ball proceeds down the barrel, so that T is constant. Third, neglect the losses: Suppose that there is no friction between the barrel and the sliding ball, but at the same time assume the ball fits tightly enough that there is no leakage of gas around it [3]. (Historically, lead shot would often be wrapped with linen to prevent gas from escaping while minimizing the coefficient of friction.) Also suppose that the atmospheric back pressure on the ball can be ignored compared to the forward gas pressure.

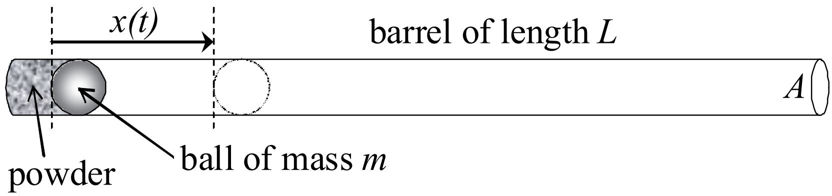

Figure 1. Ball in the Barrel of a Musket.

The gas pressure P is then related to the net force F on the ball by the definition of pressure as force per unit area, $P = F / A = ma / A$, where a is the acceleration of the ball along the barrel using Newton's second law. Furthermore, the volume of the gas is given by $V = Ax$ where x is the displacement of the ball (cf. Figure 1), and thus $PV = max$. Treating the gas as ideal, *i.e.*, $PV = nRT$ where R is the gas constant, it follows that

$$xa = kt \tag{2}$$

using Equation (1), where k is the positive constant

$$k = \frac{rRT}{m}. \tag{3}$$

Substituting $a \equiv d^2 x / dt^2$, Equation (2) becomes a nonlinear inhomogeneous differential equation for the position of the ball as a function of time, $x(t)$. A particular solution of it can be immediately found using the trial form

$$x = Bt^N \tag{4}$$

where B and N are constants to be determined. By substituting Equation (4) into (2) and equating both the powers and prefactors of t on the two sides of the equation, one finds

$$N = \frac{3}{2} \quad \text{and} \quad B = \sqrt{\frac{4k}{3}}, \tag{5}$$

so that

$$x = \left(\tfrac{4}{3}k\right)^{1/2} t^{3/2} . \tag{6}$$

The first and second time derivatives of this result give the velocity and acceleration of the ball as a function of time,

$$\upsilon = \sqrt{3kt} \tag{7}$$

and

$$a = \sqrt{\frac{3k}{4t}} . \tag{8}$$

Equation (6) is not the general solution of Equation (2) because it does not include two arbitrary integration constants. Instead it is the particular solution corresponding to $x_0 = 0$ and $\upsilon_0 = 0$ (which happily is the case most relevant to a ball in a musket). Later in this article we will consider how to find solutions for other initial conditions (see the section, "General Solution of the Differential Equation," below).

The ball is in the barrel during the time interval from $t = 0$ until some later time $t = t_{\max}$. Equations (6) and (7) then imply that the length of the barrel is

$$L = \left(\tfrac{4}{3}k\right)^{1/2} t_{\max}^{3/2} \tag{9}$$

and the muzzle velocity of the ball is

$$\upsilon_{\max} = \sqrt{3kt_{\max}} . \tag{10}$$

Equations (9) and (10) are two equations in two unknowns (k and $t_{\max}$) if L and $\upsilon_{\max}$ are measured. For example, the 58 Springfield musket [4] has a barrel length of 1 m and a muzzle velocity of 290 m/s, from which one deduces that $k = 5.4\ \mathrm{km}^2/\mathrm{s}^3$ and $t_{\max} = 5.2\ \mathrm{ms}$. Equations (6) to (8) are plotted in Figure 2 for these values. Although the acceleration initially diverges, the velocity and position are nevertheless well defined at all times. The rise in the velocity quickly tapers off, demonstrating that there is little advantage in increasing the barrel length past a certain point. (In particular, if losses were included, there would be some definite optimal length for a given powder charge.)

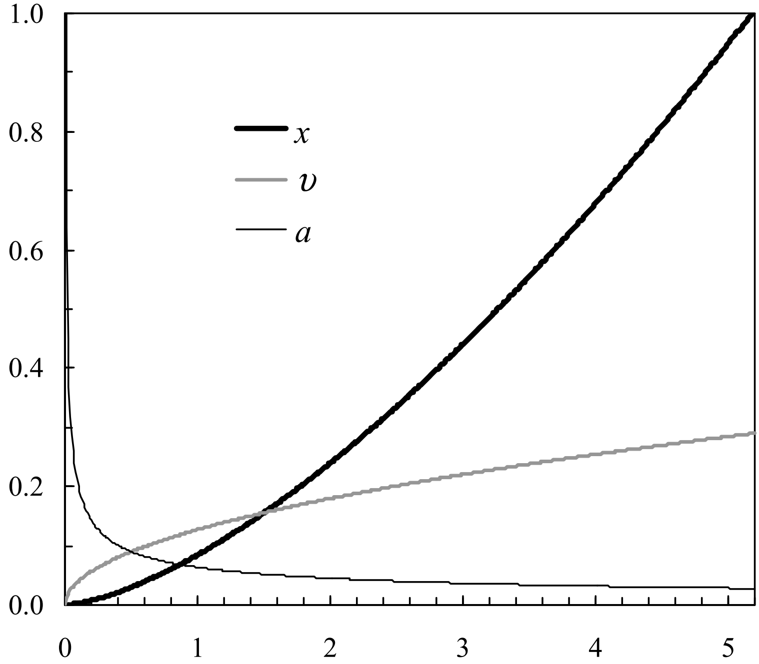

Figure 2. Graphs of x (in m), υ (in km/s), and a (in m/ms^2) versus t ranging from 0 to 5.2 ms if $k = 5.4\ \text{km}^2/\text{s}^3$ for the initial conditions $x_0 = 0$ and $\upsilon_0 = 0$.

Energetics of the Powder, Gas, and Projectile

The derivation of Equation (2) above depends on the fact that nRT increases linearly with time t. Specifically, it was assumed that T is constant and that $n = rt$. Hot gas is created (starting from zero moles) by chemical conversion of the solid powder. For simplicity, consider the gas to be monatomic. An alternative way to model the system is to take n to be constant, while $T = rt$, *i.e.*, the temperature is no longer constant. One could now think of the gas atoms as initially existing latently in the gunpowder in condensed form (which classically corresponds to absolute zero temperature) and that they get rapidly warmed up by thermal energy transfer Q from the burning charge.

Reversible thermodynamics can be used in the analysis because the gas expansion is quasistatic and there are no dissipative losses. Appendix A shows that the gas is always in quasi-equilibrium by treating the expansion of the gas behind the ball like the familiar example of a piston in a frictionless cylinder. The piston slides slowly compared to the speed of sound, provided that its mass is much larger than that of the gas.

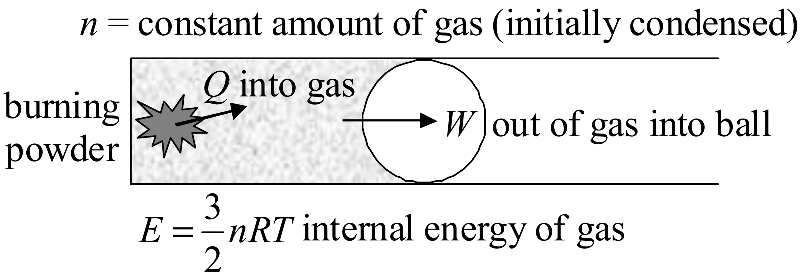

Figure 3. Relevant energy transfers between the gunpowder, propelling gas, and musket ball in the model where the number of moles n of the gas is taken to be constant and its temperature T increases linearly.

The energetics of the musket are now analyzed by reference to Figure 3. Consider an arbitrary interval of time between 0 and t. During this interval, the monatomic gas ends up with an internal energy [5] of $E(t) = 1.5nRT(t)$, whereas it started with no internal energy when condensed. Thus the change in internal energy of the propellant gas is

$$\Delta E = \frac{3}{2} nRT \,. \tag{11}$$

During this time, the gas does work W on the ball, calculated from

$$W = \int F dx = m \int a dx \tag{12}$$

(or equivalently from $\int P dV$.) One could proceed by substituting Equations (6) and (8) to convert the last result into a time integral that can be performed. A simpler and more general approach is to use the definitions of velocity and acceleration to rewrite Equation (12) as

$$W = m \int \frac{d\upsilon}{dt} \upsilon dt = \frac{1}{2} m \Delta\left(\upsilon^2\right) = \Delta K \tag{13}$$

where $K \equiv \frac{1}{2} m\upsilon^2$ is the kinetic energy of the ball. Equation (13) is simply a derivation of the work-kinetic-energy theorem of the ball since it is treated here as a particle. For the particular solution of interest (which is also the asymptotic solution for large times for any choice of initial conditions, as is proven in the section below, “Scaling Argument to Find the Asymptotic Behavior”), Equations (1), (3), and (7) can be substituted into this result to obtain

$$W = \frac{3}{2} nRT . \tag{14}$$

Finally, the first law of thermodynamics applied to the gas implies that

$$\Delta E = Q - W \quad \Rightarrow \quad Q = 3nRT \tag{15}$$

using Equations (11) and (14). In words, these results prove that energy is being transferred from the powder to the gas and projectile at the constant rate $dQ/dt = 3nRr$. Half of that added energy goes into warming up the gas, increasing its internal energy, while the other half goes into accelerating the ball, increasing its translational kinetic energy. Thus the energy transfer efficiency from the powder to the ball is 50% even for this ideal musket.

General Solution of the Differential Equation

In this section we explore the nonlinear differential equation $xa = kt$ from a more general mathematical point of view. The physical application presented above helps interpret these general numerical results.

Reparameterizing the Equation

Equation (2) is second order and so its general solution must contain two constants of integration, corresponding to the initial position x_0 and initial velocity v_0, in addition to the adjustable value of k. In total, there are thus three parameters in the family of solutions. However, some of these parameters can be eliminated by rescaling the units of length and time. This reparameterization is performed in different ways, depending on the initial conditions.

Choose the $+x$ axis to point in the direction of motion of the particle at long times. Then for $k > 0$, the position of the particle can never be negative. Appendix B discusses what happens if the ball is launched toward the origin and shows that x cannot reach (or cross) zero no matter how large the initial speed is. The particle is repelled from the origin and must eventually move in the positive x direction, either because it initially started moving in that direction or because it reversed direction after exactly one bounce.

Therefore, at times t other than zero, the position x must always be strictly positive. In contrast, at $t = 0$ the initial position x_0 can be either positive or zero. For example, Equation (2) indicates that x_0 can be nonzero if the initial acceleration is zero, whereas Equation (6) applies to the special case $x_0 = 0$. If $x_0 = 0$, then the initial velocity υ_0 cannot be negative, because otherwise the particle would thereafter move in the direction of negative x, contrary to our choice of axis. The various possible initial conditions can therefore be divided into three classes.

Class A: x_0 is positive and υ_0 is arbitrary

Define a characteristic length $\tilde{x} \equiv x_0$ and a characteristic time $\tilde{t} \equiv x_0^{2/3} k^{-1/3}$. These two quantities can be used to define a characteristic speed $\tilde{\upsilon} \equiv \tilde{x} / \tilde{t} = x_0^{1/3} k^{1/3}$ and a characteristic acceleration $\tilde{a} \equiv \tilde{x} \big/ \tilde{t}^2 = x_0^{-1/3} k^{2/3}$. In effect, the units of distance and time have been chosen to scale away x_0 and k, reducing the three-parameter family of solutions to a form that depends only on υ_0.

Class B: x_0 is zero but υ_0 is positive

Now define the characteristic length as $\tilde{x} \equiv \upsilon_0^3 k^{-1}$ and the characteristic time as $\tilde{t} \equiv \upsilon_0^2 k^{-1}$. Then the characteristic speed is $\tilde{\upsilon} \equiv \tilde{x} / \tilde{t} = \upsilon_0$ and the characteristic acceleration is $\tilde{a} \equiv \tilde{x} \big/ \tilde{t}^2 = \upsilon_0^{-1} k$. That is, the units of distance and time have been chosen to eliminate υ_0 and k. Given that $x_0 = 0$, the family of solutions to Equation (2) reduces to zero adjustable parameters with two specified initial conditions.

Class C: both x_0 and υ_0 are zero

In this case, there is only one parameter in the original problem and so we cannot independently define both a characteristic length and time. Arbitrarily choosing $\tilde{x} \equiv 1\ \text{m}$ in base SI units, then $\tilde{t} \equiv \tilde{x}^{2/3} k^{-1/3}$, $\tilde{\upsilon} = \tilde{x}^{1/3} k^{1/3}$, and $\tilde{a} \equiv \tilde{x}^{-1/3} k^{2/3}$. This class corresponds to the particular solution already found in the first section of this paper, "Basic Dynamics of the Ball in a Musket."

For any of the three classes, dimensionless kinematic variables can be introduced as $t' \equiv t/\tilde{t}$, $x' \equiv x/\tilde{x}$, $\upsilon' \equiv \upsilon/\tilde{\upsilon}$, and $a' \equiv a/\tilde{a}$. In terms of these dimensionless variables, Equation (2) becomes

$$x'a' = t' \tag{16}$$

where $\upsilon' = dx'/dt'$ and $a' = d\upsilon'/dt'$. The initial conditions for class A are $x_0' = 1$ and $\upsilon_0' = x_0^{-1/3}k^{-1/3}\upsilon_0$. The differential equation has thus been recast in a form that only depends on the single combined value υ_0'. That makes it easier to investigate and plot its family of solutions. For class B, the initial conditions are uniquely specified as $x_0' = 0$ and $\upsilon_0' = 1$. Using l'Hôpital's rule, the initial acceleration is then $a_0' = 1$.

Numerical Solution

Equation (16) has no discernible closed-form analytic solution in general, but one can numerically integrate it. Different methods can be used for this purpose, depending on the desired accuracy and ease of calculations. To start with, the first-order Euler-Cromer method [6] can be implemented in a spreadsheet. Given values x_i' and υ_i' at any time t_i', their values at the next time step $t_{i+1}' = t_i' + \Delta t'$ (where $\Delta t' = 0.1$ say, corresponding to a time step in real units of $\tilde{t}/10$) are sequentially calculated as

$$\begin{aligned} \upsilon_{i+1}' &= \upsilon_i' + a_i'\Delta t' = \upsilon_i' + \left(t_i'/x_i'\right)\Delta t' \\ x_{i+1}' &= x_i' + \upsilon_{i+1}'\Delta t' \end{aligned} \tag{17}$$

with starting values for class A of $t_0' = 0$, $x_0' = 1$, and any chosen value of υ_0'. The results are plotted as the solid curves in Figure 4 for four values of υ_0'. A similar numerical integration for class B (when $x_0' = 0$, $\upsilon_0' = 1$, and $a_0' = 1$) results in a curve that is almost indistinguishable from the dashed curve (corresponding to class C).

The equation for x_{i+1}' involves the updated velocity υ_{i+1}' rather than the previous value υ_i', in contrast to the equation for υ_{i+1}' which uses the previous value of the acceleration a_i'. That is the hallmark of Cromer's modification of the standard Euler method, classified as a symplectic integrator. Symplectic methods are the preferred choice when the Lagrangian L has no explicit time dependence, but they can be used even when L is time dependent (as is shown in Appendix C to be the case here). By comparison with the results of the second-order leapfrog integration in Appendix D, the Euler-Cromer method obtains values of position and velocity that are found to be accurate to 0.4% or better, so Equation (17) suffices to generate Figure 4.

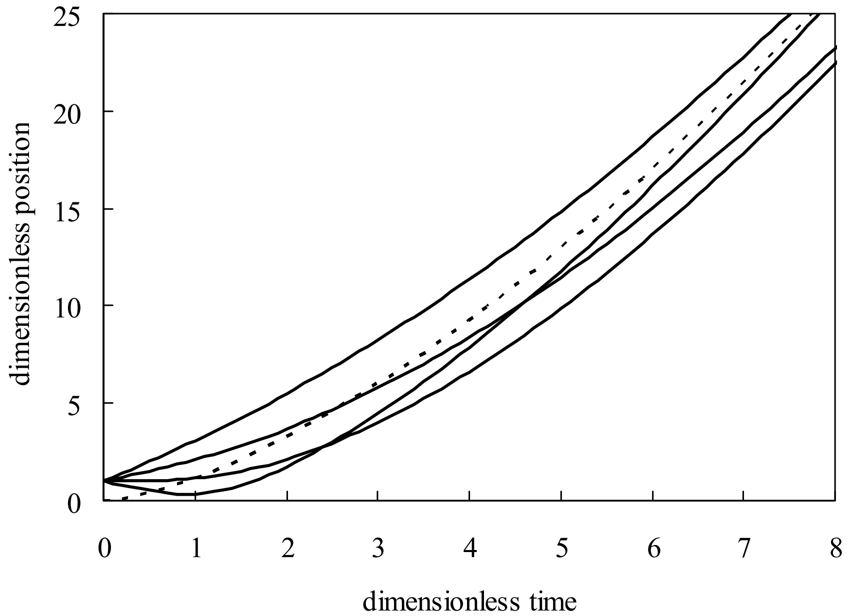

Figure 4. Graphs of x' versus t'. The four solid curves were calculated numerically using Equation (17) for $x_0' = 1$ and υ_0' equal to 2, 1, 0, and –1 (from top to bottom at $t' = 1$). The dashed curve is a plot of Equation (18).

Scaling Argument to Find the Asymptotic Behavior

The dashed curve in Figure 4 is a plot of the solution represented by Equation (6) in dimensionless form,

$$x' = \sqrt{\tfrac{4}{3}}\, t'^{3/2} \tag{18}$$

which is the particular solution of Equation (16) for class C, *i.e.*, initial values $x'_0 = 0$ and $\upsilon'_0 = 0$. To investigate how Equation (18) relates to the numerical results in the "Numerical Solution" section above, introduce new variables $x'' \equiv x' / s^3$ and $t'' \equiv t' / s^2$ where s is an arbitrary positive scaling factor that zooms Figure 4 in or out (albeit not equally for the two axes). Defining $\upsilon'' \equiv dx'' / dt''$ and $a'' \equiv d^2 x'' / dt''^2$, Equation (16) becomes

$$x'' a'' = t'' \tag{19}$$

with initial conditions $x''_0 = x'_0 / s^3$ and $\upsilon''_0 = \upsilon'_0 / s$. Then if $s \to \infty$, the solution corresponding to $x''_0 = 0$ and $\upsilon''_0 = 0$ is obtained, namely $x'' = (4/3)^{1/2} t''^{3/2}$. Therefore Equation (18) is an asymptotic solution of Equation (16) at large times for *any* initial values. To verify that conclusion, Figure 4 was replotted with the range of t' values increased 25-fold. On this expanded scale, the solid curves are indistinguishable by eye from the dashed curve.

Oscillations about the Asymptotic Solution

To quantify the manner in which the general solutions approach the asymptotic curve, dimensionless residuals $\Delta x'$ are computed by subtracting the analytic particular solution given by Equation (18) from any solution $x'(t')$ computed numerically. Whenever a numerical solution has a smaller value of x' (at a given t') than the asymptotic solution, it has a larger acceleration (*i.e.*, second derivative), and vice-versa, according to Equation (16). The numerical solution thus repeatedly catches up to and crosses the asymptotic curve, oscillating about it. It is found that these oscillations have both increasing period and increasing absolute amplitude.

A physical explanation for these oscillations can be found in the ballistic situation of the first section, "Basic Dynamics of the Ball in a Musket." If the ball gets ahead of the position it has in the particular solution at the same time, the gas becomes under-pressured in comparison and the ball's acceleration drops. That permits the gas pressure to "catch up," but the inertia of the ball leads to an overcorrection, and the cycle now reverses.

Returning to the residuals, the amplitude of $\Delta x'$ is proportional to $\sqrt{t'}$ as $t' \to \infty$, according to the analysis in Appendix D. Therefore the *relative* amplitude of the oscillations, $\Delta x'/x'$, decreases to zero in proportion to $1/t'$ for large times. In this relative sense, solutions of Equation (16) for any initial conditions converge onto the asymptotic solution, Equation (18).

Conclusions

The force law described by $xa = kt$ has a simple form but exhibits rich behavior. Physically, it describes the idealized motion of a ball in an unrifled musket. Another situation that gives rise to Equation (2) is the radial motion of a particle (of mass *m* and charge *q*) in the electric field of a long straight wire whose linear charge density is proportional to time, $\lambda = \alpha t$. Then $k = \alpha q / 2\pi e_0 m$ (where e_0 is the permittivity of free space), which allows the possibility of a negative value of *k* that the ballistic application does not. Investigation of the motion for $k < 0$ could make an interesting student project. Further study of the equation $a \propto t/x$ may uncover additional applications and intriguing behavior.

Mathematically, the solution of Equation (2) involves power-law behavior (of the particular solution), oscillatory behavior (of the residuals), and exponential behavior (of the intervals between zero crossings of the oscillations). It calls for a diverse combination of analysis techniques, including insights from physics, trial solutions of differential equations, scaling laws, graphical methods, algebraic approximations, and computational algorithms.

Appendix A: Quasistatic Expansion of the Gas Pushing the Ball in the Barrel

At long times (if not initially), the speed of the musket ball is given by the slope of the dashed curve in Figure 4, obtained by substituting Equation (3) into (7) to get

$$\upsilon_{\text{ball}} = \sqrt{\frac{3nRT}{m_{\text{ball}}}} \tag{A.1}$$

after replacing $n = rt$ from Equation (1). Here the subscript “ball” has been added to υ and *m* to emphasize that those two variables refer to the speed and mass of the projectile specifically. On the other hand, the root-mean-square speed of the atoms in a monatomic ideal gas is known from kinetic theory or equipartition [5] to be

$$\upsilon_{\text{gas}} = \sqrt{\frac{3nRT}{m_{\text{gas}}}} \tag{A.2}$$

where m_{gas} is the total mass of the gas in the musket. (The speed of sound has almost the same value, obtained by replacing the factor of 3 in this equation by the adiabatic exponent $\gamma = 5/3$.) Comparing Eqs. (A.1) and (A.2), one sees that the speed of the ball will always be small compared to typical molecular speeds provided that the mass of the ball is much larger than the total mass of the gas. In that case, the gas expansion is said to be quasistatically slow.

Appendix B: Motion of the Ball for Negative Initial Velocities

One cannot compress the volume of the gas in the barrel to zero (at nonzero temperatures). However, if one runs the Euler-Cromer simulation specified by Equation (17) with say $\upsilon'_0 = -3$ and $\Delta t' = 0.1$, the trajectory appears to cross the horizontal axis (near $t' = 0.34$) and become increasingly negative thereafter. This zero crossing is an artifact of inaccurate numerical integration. It only occurs when the time step is large enough that the simulation can "jump" over the divergence in the repulsion that occurs at $x' = 0$. We can prove that such a jump does not occur for infinitesimally fine time steps as follows.

Consider the specific work, i.e., work per unit mass, $\int a'dx'$ as the ball approaches $x' = 0$. Then t' is approximately constant (for example at about 0.34 if $\upsilon'_0 = -3$) during the small time interval that x' is smaller than some initial value x'_{i}, say 0.1. Now according to the work-kinetic-energy theorem,

$$\upsilon'^2 - \upsilon_{\text{i}}'^2 = 2\int_{x'_{\text{i}}}^{x'} a'dx' \approx 2t' \ln \frac{x'}{x'_{\text{i}}} \tag{B.1}$$

using Equation (16). The right-hand side of this equation is negative (because $x' < x'_{\text{i}}$) and thus the ball slows down as it approaches $x' = 0$. But it can never reach $x' = 0$ because the left-hand side can never get smaller than $-\upsilon_{\text{i}}'^2$ in value. Consequently, even if the negative initial velocity is very large in magnitude, the ball will necessarily bounce off the (infinite) potential barrier at the origin, as occurs for the curve corresponding to

$\upsilon_0' = -1$ in Figure 4.

Appendix C: Canonical Mechanics of the System

An explicitly time-dependent Lagrangian L and Hamiltonian H can be constructed as follows. Equation (B.1) suggests a potential energy $U(t)$ that is logarithmic in the position and thus

$$L \equiv K - U = \tfrac{1}{2} m\dot{x}^2 + mkt \ln x \tag{C.1}$$

where $\dot{x} \equiv \upsilon$. The momentum conjugate to the position x is

$$p \equiv \frac{\partial L}{\partial \dot{x}} = m\dot{x} \tag{C.2}$$

and thus the Hamiltonian is

$$H \equiv p\dot{x} - L = \tfrac{1}{2} m\dot{x}^2 - mkt \ln x \,. \tag{C.3}$$

Then the equation of motion is obtained from Hamilton's equation as

$$\dot{p} = -\frac{\partial H}{\partial x} \quad \Rightarrow \quad m\ddot{x} = \frac{mkt}{x} \tag{C.4}$$

which rearranges into $xa = kt$. Alternatively, this equation of motion can be obtained from Equation (C.1) using the Lagrange equation

$$\frac{d}{dt}\frac{\partial L}{\partial \dot{x}} = \frac{\partial L}{\partial x} \,. \tag{C.5}$$

Appendix D: Harmonic Oscillations of the Residuals

Dropping the primes so as to unclutter the notation, the dimensionless force law is

$$\ddot{x} = \frac{t}{x} \tag{D.1}$$

from Equation (16), with a particular solution of

$$x_{\mathrm{p}} = \sqrt{\tfrac{4}{3}}\, t^{3/2} \,. \tag{D.2}$$

Define the residual Δx as the difference between a general solution of

Equation (D.1) for x and the right-hand side of Equation (D.2). Examination of numerical results from Equation (17) suggests that the residual (for any value of the dimensionless initial velocity υ_0) oscillates harmonically in the logarithm of the elapsed time t with an amplitude that increases in proportion to the square root of the time. To verify this suggestion, let the scaled residual z be defined as Δx divided by $\sqrt{t}$, so that

$$z = xt^{-1/2} - \sqrt{\tfrac{4}{3}}\, t \tag{D.3}$$

which can be solved for x to get

$$x = zt^{1/2} + \sqrt{\tfrac{4}{3}}\, t^{3/2} . \tag{D.4}$$

Take the second derivative of this equation with respect to time, and substitute both it and Equation (D.4) into (D.1) to obtain

$$\left(1 + \sqrt{\tfrac{3}{4}}\, z/t\right)^{-1} = 1 + \sqrt{\tfrac{4}{3}}\left(\ddot{z}t + \dot{z} - \tfrac{1}{4} z/t\right). \tag{D.5}$$

Since it will be shown that the amplitude of the scaled residual z levels off in value asymptotically (cf. Figure 5), z/t must approach zero for large t. Thus the left-hand side of Equation (D.5) can be approximated using the binomial expansion to first order. The result can be rearranged to get

$$\ddot{z}t^2 + \dot{z}t = -\tfrac{1}{2} z . \tag{D.6}$$

The left-hand side of this equation can be identified as the logarithmic second derivative

$$\frac{d^2 z}{(d \ln t)^2} = \ddot{z}t^2 + \dot{z}t . \tag{D.7}$$

Therefore Equation (D.6) implies that the (logarithmic) second derivative of z is proportional to $-z$, characteristic of simple harmonic motion. Consequently the residual oscillates semi-logarithmically with a period of $2\pi\sqrt{2}$, *i.e.*, a half-period corresponds to a ratio of adjacent zero-crossings of $z(t)$ that equals $\exp\left(\pi\sqrt{2}\right) \approx 85.02$.

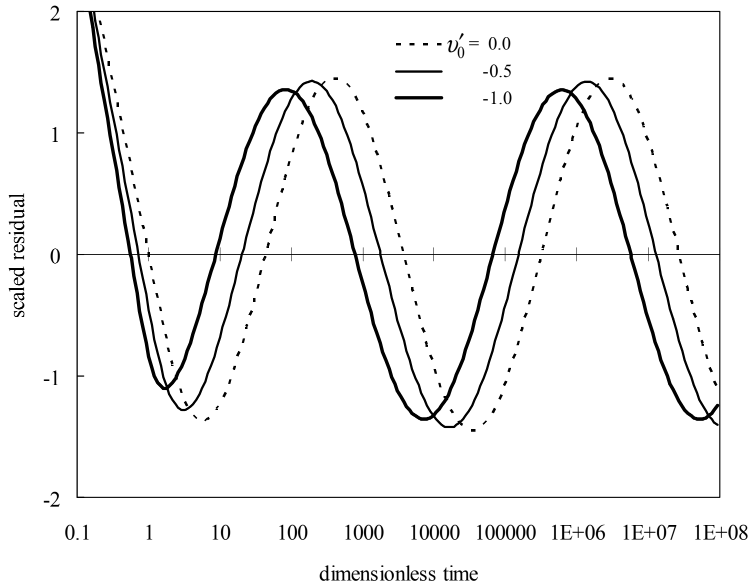

Figure 5. Semi-logarithmic plots of the scaled residual $\Delta x'/\sqrt{t'}$ against the dimensionless time t' for the three indicated values of v_0' with $x_0' = 1$.

Figure 5 plots the scaled residual z as a function of time on semi-logarithmic axes for $x_0 = 1$. The three curves correspond to different values of v_0 between 0 and –1. Zero crossings for these three curves are listed in Table 1. For large t, the ratio between successive zero crossings is in excellent agreement with the asymptotic value 85.02 predicted by Equation (D.6).

The results in Table 1 require x values accurate to better than 1 part in 10^9, because z is a small difference between large numbers. To achieve that level of accuracy, a C++ program [7] was written to calculate the residuals over a longer range of times and with higher accuracy than can be done using the spreadsheet solution. The program replaces the first-order calculations of Equation (17) with the second-order leapfrog calculations

$$x_{i+1} = x_i + v_i \Delta t + \frac{1}{2}\left(\frac{t_i}{x_i}\right)(\Delta t)^2 \quad \text{and} \quad v_{i+1} = v_i + \frac{1}{2}\left(\frac{t_i}{x_i} + \frac{t_{i+1}}{x_{i+1}}\right)\Delta t\,. \quad \text{(D.8)}$$

An adaptive time step size is used: Δt is gradually increased as t increases, to keep pace with the exponential increase in the period of oscillations. An even higher-order symplectic integrator [8] was used as a further check on the results.

Table 1. Zero-crossing times in Figure 5 and their ratios, accurate to 1 part in 10^4, for three different values of the dimensionless velocity.

for $v_0' = -1.0$:		for $v_0' = -0.5$:		for $v_0' = 0.0$:	
zero-crossing time	ratio	zero-crossing time	ratio	zero-crossing time	ratio
8.7402		20.493		43.493	
	89.47		87.02		85.98
781.99		1783.2		3739.5	
	84.97		85.00		85.01
66 446		151 570		317 890	
	85.02		85.02		85.02
5 649 300		12 886 000		27 027 000	

Acknowledgment

We thank John Mallinckrodt for discovering that the numerical solutions oscillate about the asymptotic curve and for the ideas presented in Appendix B.

This paper won the Frank R. Haig prize at the Chesapeake Section of the American Association of Physics Teachers at the Spring 2012 Capital Science meeting

References

[1] M. Denny, *Their Arrows Will Darken the Sun: The Evolution and Science of Ballistics* (Baltimore, Johns Hopkins University Press, 2011) Technical Note 7.

[2] M. Denny, "The internal ballistics of an air gun," *Phys. Teach.* **49**, 81–83 (2011).

[3] C.E. Mungan, "Internal ballistics of a pneumatic potato cannon," *Eur. J. Phys.* **30**, 453–457 (2009).

[4] http://www.hackman-adams.com/guns/58musket.htm .

[5] R. Feynman, R.B. Leighton, and M.L. Sands, *The Feynman Lectures on Physics* (Reading, Addison-Wesley, 1963) Vol. I.

[6] A. Cromer, "Stable solutions using the Euler approximation," *Am. J. Phys.* **49**, 455–459 (1981).

[7] http://usna.edu/Users/physics/mungan/Publications/ratio-gun-eom.c .

[8] E. Hairer, C. Lubich, and G. Wanner, *Geometric Numerical Integration: Structure-Preserving Algorithms for Ordinary Differential Equations*, 2nd ed. (Berlin, Springer, 2006) with codes online at http://www.unige.ch/~hairer/software.html.